Carbohydrate Polymers 109 (2014) 139–147

Contents lists available at ScienceDirect

Carbohydrate Polymers

journal homepage: www.elsevier.com/locate/carbpol

ZnO-modified cellulose fiber sheets for antibody immobilization

Vinay Khatri[a,b], Katalin Halász[a], Lidija V. Trandafilović[c], Suzana Dimitrijević-Branković[d], Paritosh Mohanty[b], Vladimir Djoković[c,*], Levente Csóka[a]

[a] University of West Hungary, Institute of Wood Based Products and Technologies, Bajcsy Zs. E. u. 4, 9400 Sopron, Hungary
[b] Department of Applied Science and Engineering, Indian Institute of Technology, Roorkee, Saharanpur Campus, Saharanpur 247001, India
[c] Vinča Institute of Nuclear Sciences, University of Belgrade, P.O. Box 522, 11001 Belgrade, Serbia
[d] Department of Bioengineering and Biotechnology, Faculty of Technology and Metallurgy, University of Belgrade, Karnegijeva 4, 11120 Belgrade, Serbia

ARTICLE INFO

Article history:
Received 25 November 2013
Received in revised form 15 March 2014
Accepted 18 March 2014
Available online 1 April 2014

Keywords:
Antibody immobilization
Cellulose
Fibers
ZnO
Antimicrobial properties
Bioactive paper

ABSTRACT

Cellulose fiber sheets impregnated with saccharide capped-ZnO nanoparticles were used as bioactive materials for antibody immobilization. First, ZnO nanoparticles were synthesized in the presence of glucose (monosaccharide), sucrose (disaccharide) as well as alginic acid and starch (polysaccharides). The pine cellulose fibers were then modified by the obtained saccharide capped nanoparticles and further incorporated into the sheets. The presence of ZnO significantly improved the immobilization of the antibodies on the surface of the sheets. After rewetting the alginic acid-ZnO modified sheets with saline solution, the retention of antibodies was about 95%. A high degree of the immobilization of biomolecules is an important feature for possible fabrications of bioactive- or biosensing-papers and we successfully tested the sheets on the detection of blood types using (A, B, and D blood antibodies). The ZnO nanoparticles affected also the other properties of the sheets. The ZnO-modified fiber sheets showed higher values of tensile index (strength), smoothness and opacity, while the value of porosity was substantially lower than that of the unmodified sheet. The presence of ZnO nanoparticles provided also the antimicrobial activity to the sheets. They showed a strong activity against bacteria (*Escherichia coli* and *Staphylococcus aureus*) and strong resistance to the attack of cellulase producing fungus *Gloeophyllum trabeum*.

1. Introduction

A paper has traditionally been defined as a felted sheet formed on a fine screen from a water suspension of cellulose fibers (Thorp & Kocurek, 1991). It is indispensable in our daily life having an immense number of applications. However, as a result of current trends toward exploitation of renewable and eco-friendly materials, the applications of paper expanded also to the domains previously dominated by synthetic plastics (Jain et al., 2013). The cellulose fibers are inexpensive, biodegradable, easy to use and readily available so the paper based products became very attractive for food packaging. At the same time, organic, hydrophilic and highly porous nature of paper makes it prone to attack by microorganisms. One of the methods suggested to address this problem is to modify the paper using inorganic nanoparticles such as ZnO and Ag that exhibit strong microbicidal properties (Csóka et al., 2012; Ghule, Ghule, Chen, & Ling, 2006; Gottesman et al., 2011; Prasad et al., 2010). In our previous study (Csóka et al., 2012), we showed that the silver nanoparticles, besides providing the antimicrobial activity to cellulose fiber sheets, improved also their mechanic and viscoelastic properties. Here, we make one step further and investigate whether the presence of the ZnO nanoparticles (surface modified with different saccharides) can also improve the ability of the cellulose sheets to immobilize antibodies.

ZnO is a wide band gap (E_g = 3.37 eV) metal oxide with good catalytic, electrical and photochemical properties (Ashour, Kaid, Elsayed, & Ibrahim, 2006; Brida et al., 2002; Wang, 2004). It has a high isoelectric point (IEP) hence it can adsorb or immobilize the biomolecules (enzymes, proteins or antibodies) having a low IEP (Umar, Rahman, Al-Hajry, & Hahn, 2009). ZnO exhibits strong antimicrobial activity that most probably originates from the generation of H_2O_2 on its surface (Applerot et al., 2009; Jones, Ray, Ranjit, & Manna, 2008; Trandafilović, Božanić, Dimitrijević-Branković, Luyt, & Djoković, 2012). On the other hand, the toxicity of ZnO to human cells is quite low and, what is even more important; it does not significantly increase in potency when nanostructured particles were used instead of conventional ZnO powders (Moos et al., 2011). Since the toxicity is, more or less, unaffected by the particle size, we decided to use nanoparticles due

* Corresponding author. Tel.: +381 113408538; fax: +381 113408607.
E-mail addresses: djokovic@vinca.rs, vladimirdjokovic@hotmail.com (V. Djoković).

http://dx.doi.org/10.1016/j.carbpol.2014.03.061
0144-8617/

to their higher surface activities. Of course, the decrease in size of the particles is followed by an increase in surface energy and they showed pronounced agglomeration. To minimize this effect, we adopted recent strategies of using of mono-, di- and polysaccharide based capping agents for stabilization of the growth of inorganic nanoparticles. Because of a large number of hydroxyl groups, the saccharide molecules complex well with metal ions and provide a stable environment for the growth of metal, metal-oxide and metal-sulfide nanoparticles. Monosaccharides (glucose, galactose), disaccharides (maltose and lactose) (Pancek et al., 2006), and polysaccharides, (dextran (Walsh, Arcelli, Ikoma, Tanaka, & Mann, 2003), starch (Bozanic et al., 2007; Radhakrishnan, Georges, Nair, Luyt, & Djoković, 2007; Raveendran, Fu, & Wallen, 2003; Vigneshwaran, Kumar, Kathe, Varadarajan, & Prasad, 2006), carboxymethyl cellulose (Chang, Yu, & Ma, 2009; Yu, Yang, Liu, & Ma, 2009), glycogen (Bozanic, Dimitrijevic-Brankovic, Bibic, Luyt, & Djokovic, 2011; Božanić, Luyt, Trandafilović, & Djoković, 2013), chitosan (Murugadoss & Chattopadhyay, 2008; Perelshtein et al., 2013; Shih, Shieh, & Twu, 2009), and alginic acid (Chang, Yu, Ma, & Anderson, 2011; Trandafilović et al., 2012)), proved to be excellent stabilization agents for inorganic nanoparticles.

In this study, the ZnO nanoparticles were prepared by using four different carbohydrates (monosaccharide: glucose, disaccharide: sucrose and polysaccharides: alginate and starch) as capping agents. The former procedure enabled an easy attachment of the nanoparticles onto the surface of cellulose fibers, which are further used for the preparation of the cellulose sheets. Our aim was to investigate the influence of the ZnO nanoparticles on the properties of the sheets and to establish if these properties are affected by changing the molecular mass of the saccharides used to cap the nanoparticles. The focus will be on the ability of the modified sheets to immobilize biomolecules, which will be tested on three types of blood antibodies (A, B and D). Since the polysaccharides are biocompatible, non-toxic and cost effective, we believe that in this way prepared ZnO impregnated sheets can be useful for various biological applications. The present investigations, in particular, are directed toward development of bio-active paper. They are in line with recent trends of using paper as supporting material for biological components that are capable to identify, capture and/or inactivate specific analyte molecules such as pollutants, antigens, pathogens, drugs, allergens, etc. (Abe, Suzuki, & Citterio, 2008; Ali et al., 2009; Hossain et al., 2009; Li, Tian, Nguyen, & Shen, 2008). On the other hand, for the application of bioactive cellulose fiber sheets, the retention of biomolecules (antibodies or enzymes) is essential. It was shown that the polymers can be used as retention aids in order to increase the initial enzyme concentration on the paper and their retention upon rewetting (Khan, Haniffa, Slater, & Garnier, 2010). We intend to show that this can also be achieved by impregnation of the sheets with saccharide modified ZnO nanoparticles. In addition, we will report on the effects of the nanoparticles on mechanical and antimicrobial properties of the sheets.

2. Materials and methods

2.1. Materials and sample preparation

Bleached pine cellulose fibers were received from Robert Placzek GmbH. Glucose, sucrose, starch, alginic acid, zinc acetate and sodium hydroxide were received from Sigma Aldrich. Anti-A (A-mono-11H5 clones), Anti-B (B-mono-6F9 clones) and Anti-D blended IgG/IgM (D-mono-blend-TH 28 clones) antibodies were purchased from CE-Immundiagnostika GmbH, while Bradford protein assay of Coomassie Brilliant Blue G-250 (Bradford Reagent) was obtained from Sigma Aldrich.

2.1.1. Preparation of glucose-, sucrose-, alginic acid- and starch–ZnO modified nanoparticles

The carbohydrate solutions were prepared by dissolving 1 g of respective carbohydrates (glucose, sucrose, alginic acid and starch) into 100 mL of 0.01 M sodium hydroxide solution. The procedure for the preparation of saccharide modified ZnO nanoparticles is based on our recent study on ZnO–alginate nanocomposites (Trandafilović et al., 2012). Briefly, 2 mL of 0.2 M Zn–acetate solution was mixed with 0.8 mL of 1 M sodium hydroxide solution. Into that mixture, 5 mL of 1% of carbohydrate solution was added drop by drop. After that, the mixtures were treated at 800 W for 30 s in the microwave oven. Slow centrifugation was used to collect the obtained modified ZnO nanoparticles. The samples were washed several times with distilled water and dried at 40 °C. Depending on the saccharide material used in preparation, the samples were denoted as G-ZnO (glucose), S-ZnO (sucrose), AA-ZnO (alginic acid) and St-ZnO (starch).

2.1.2. Modification of cellulose fibers with saccharide modified ZnO-nanoparticles

The ZnO nanoparticle solutions were mixed with the suspension of cellulose fibers (3 g of fibers in 300 ml of water). The amount of G-ZnO, S-ZnO, AA-ZnO and St-ZnO dry materials with respect to amount of fibers was 0.1 wt.% (0.001 g of modified ZnO nanoparticles per gram of fibers).

2.1.3. Preparation of cellulose fiber sheets with incorporated ZnO nanoparticles

Before making the hand sheet, the fibers were beaten up to 35 Schopper-Riegler degrees (°SR) by using a commercial laboratory valley beater. HAAGE D-4330 laboratory sheet former was used for the fabrication of the unmodified and ZnO-modified hand-sheets with a grammage of 100 g m^{-2}. Prior the characterization, all the sheets were conditioned at 23 °C and 50% relative humidity (RH) for 48 h.

2.2. Methods

2.2.1. UV–vis spectroscopy

UV–vis spectra of the saccharide modified ZnO nanoparticle solutions were recorded on a WPA lightwave S2000 Diode array UV–vis spectrophotometer. For comparison, the UV–vis spectrum of the water suspension of the commercial micron size ZnO powder was also recorded.

2.2.2. X-ray diffraction (XRD)

The X-ray diffraction patterns were recorded at room temperature in the 5–80° 2θ range using an MPD Pro Panalytical diffractometer equipped with a linear Xcelerator detector. Cu-K_α (1.54056 Å) radiation was used with the 0.016° recording step and the 1000 s per step counting time.

2.2.3. Scanning electron microscopy (SEM)

SEM-HITACHI S-3400N instrument was used for SEM imaging of unmodified and ZnO-modified fibers. The images were obtained in the backscattered electrons (BSE) imaging mode at an operating voltage of 17 kV.

2.2.4. Tensile strength

Tensile strength of unmodified (Control) as well as G-ZnO, S-ZnO, St-ZnO and AA-ZnO modified cellulose sheets was measured on an INSTRON 3345 Tensile Tester according to EN ISO 1924-2 standard. The cross head speed was 50 mm/min and gap between the clamps was 180 mm. The rectangular samples 15 mm in width were used.

2.2.5. Brightness and opacity

The brightness and opacity of the prepared cellulose fiber sheets were investigated by using an Elrephodatacolor 2000 instrument. Before the measurement, the instrument was calibrated according to the TAPPI standard (T 452 om-02). The black trap and white tile were used and the monochromatic light $\lambda = 457$ nm. For the opacity measurement, the monochromatic light of $\lambda = 557$ nm was used.

2.2.6. Porosity and smoothness

The porosity and smoothness of the unmodified and ZnO modified cellulose fiber sheets were measured on a Smoothness Porosity Tester (Bendtsen Type). The smoothness of the paper describes the topography of the fiber network surface. The tester measures the resistance of the paper surface to the air stream that flows between the paper and a surface of the instrument head pressed against it. The porosity represents the ratio of pore volume to total volume of the paper and it is obtained indirectly by measuring the air permeability. The instrument measures the flow of air through the certain area of the paper caused by the pressure difference on the opposite sides of the sample.

2.3. Microorganisms and antimicrobial activity

2.3.1. Microorganisms and culture conditions

In order to study the anti-microbial activity of unmodified and ZnO-modified cellulose fiber sheets three microorganisms were used as indicator strains: Gram-negative bacteria *Escherichia coli* ATCC 25923, gram-positive bacteria *Staphylococcus aureus* ATCC 25922 and fungus *Gloeophyllum trabeum* ATCC 11539. Trypton soy broth enriched with 0.6% (v/v) yeast extract (TSBY; Institute of Immunology and Virology, Torlak, Belgrade) was used for the preservation and the growth of the bacteria. The bacteria were cultured in 3 mL TSBY at 37 °C and left overnight. The initial numbers of *S. aureus* and *E. coli* in the testing medium were 2.12×10^5 CFU mL^{-1} and 1.24×10^5 CFU mL^{-1}, respectively. The growth of fungus (*G. trabeum*) was carried out in a Malt Extract Agar. Fungal cultures were inoculated on Malt extract agar and incubated at 25 °C for 7–8 days.

2.3.2. Antibacterial activity testing

Quantitative estimation of anti-microbial activity of G-ZnO, S-ZnO, St-ZnO and AA-ZnO modified cellulose sheets was carried out in a potassium hydrogen phosphate buffer solution according to the ASTM E 2149-01 standard. Cellulose sheet samples (0.01 g by weight) were immersed in the glass tubes containing 9.9 mL of the testing solution. After that, 0.1 mL of microbial inoculum (prepared by mixing 1 mL of initial cultures with 9 mL of saline) was added. The resulting mixture was vortexed for 10 s and incubated at 37 °C in a waterbath shaker. After 1 h of exposure, 0.1 mL aliquots were separated and further diluted with sterile physiological saline solution (8.5 g NaCl in 1 L of water). From the appropriate dilutions, 0.1 mL aliquots were transferred in Petri dishes, covered with trypton soy agar (Torlak, Serbia) and incubated at 37 °C for 24 h. At the end of this period, the number of colonies of viable bacteria was determined. Calculation of bacterial reduction (R, %) was done using the following equation:

$$R = \frac{C_0 - C}{C_0} \times 100, \quad (1)$$

where C_0 (CFU – colony forming units) is the number of bacterial colonies from the control saline and C (CFU) is the number of bacterial colonies from the samples.

2.3.3. Antifungal activity testing

The ZnO-modified fiber sheets were assessed for their tolerance toward fungi infection. The samples were exposed to *G. trabeum*, which is a cellulase (Endoglucanase Cel5A) producing fungus. The tensile indexes of unmodified and (G-ZnO, S-ZnO, St-ZnO and AA-ZnO) modified cellulose sheets were measured after their exposure to fungus for 10 days.

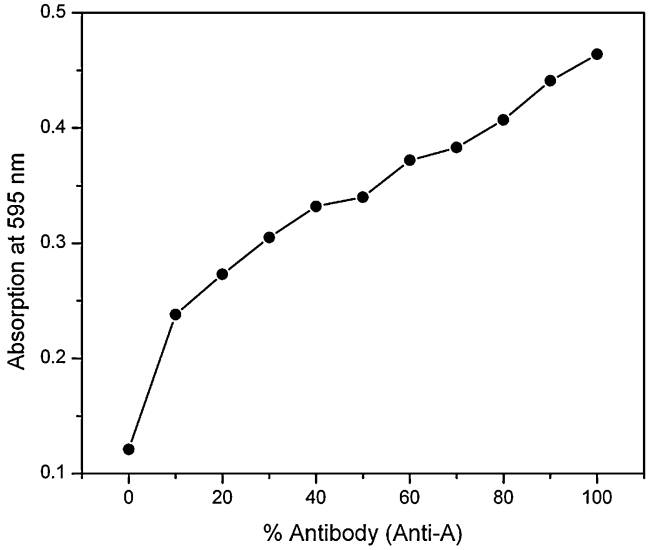

Fig. 1. A typical Bradford total protein assay calibration curve for (Anti-A) antibody.

2.4. Immobilization of antibodies on ZnO-nanoparticle modified fibers

For the study of the immobilization of biomolecules on G-ZnO, S-ZnO, St-ZnO and AA-ZnO modified cellulose sheets, a 10 mm × 10 mm square samples were used. They were treated with 3 different types of antibodies: Anti-A, Anti-B and Anti-D. The antibody solutions were poured over the paper samples using a fine pipette, which are then left to dry for 30 min. Rewetting of the bioactive cellulose fiber sheet can cause the antibody or enzyme desorption from the fiber surface. In order to study the degree of the immobilization of antibodies, after drying for 30 min, the fiber sheets were washed or rewetted with 2 mL of saline solution. The washed through saline solution was collected in cuvettes and used for quantification of desorbed antibodies. The antibodies are large glycoproteins so Bradford protein assay (Bradford reagent) can be used for their quantification (Jarujamrus et al., 2012). To test the dye-binding, 200 μL of Bradford assay was added into the cuvette with the sample and incubated for 5 min at room temperature. The changes in color of the sample solutions were measured by using UV–vis absorption spectroscopy at $\lambda = 595$ nm. The percentage of the retention was determined from Bradford total protein assay calibration curves. A typical calibration curve for (Anti-A) antibody was shown in Fig. 1.

3. Results and discussion

The mechanism of the growth of ZnO nanoparticles in the presence of polysaccharide was suggested in our previous study (Trandafilović et al., 2012). The process takes place according to following reactions:

$$Zn^{2+} + 4OH^- \rightarrow Zn(OH)_4{}^{2-}, \quad (R1)$$

$$Zn(OH)_4{}^{2-} \rightarrow ZnO + 2H_2O + 2OH^-. \quad (R2)$$

Zn^{2+} ions first react with OH^- and create the precursor $Zn(OH)_4{}^{2-}$ (reaction (R1)), which upon heating decomposes to ZnO nanoparticles (reaction (R2)). The saccharides and polysaccharides environments used in synthetic procedures enable better control of the growth of the nanoparticles. Usually, the polarity of water

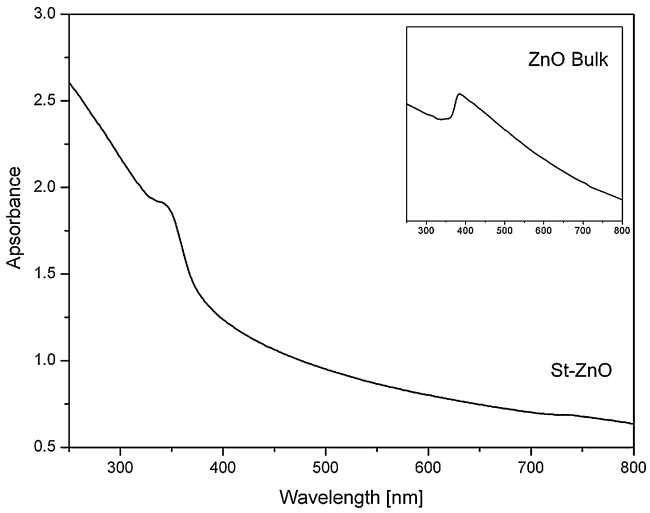

Fig. 2. UV–vis absorption spectra of the St-ZnO water solution. The inset shows the absorption spectra of the micron-size ZnO powder.

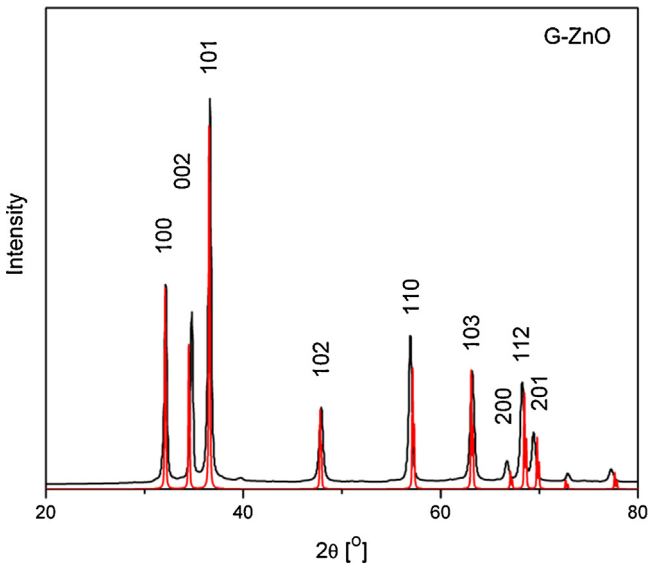

Fig. 3. XRD patterns of the G-ZnO sample and the bulk ZnO crystal.

causes the agglomeration of ZnO nanoparticles formed and their incorporation into larger particles. The saccharide biomolecules prevent to a certain extent the particle diffusion and for this reason their growth is more localized.

3.1. UV–vis absorption spectroscopy

Fig. 2 shows the UV–vis absorption spectrum of the St-ZnO solution. The UV–vis spectrum shows a dominant absorption at ~349 nm, which is shifted toward lower wavelengths with respect to the absorption peak of bulk ZnO (380 nm, inset). The former effect is obviously the consequence of exciton confinement and implies the presence of nanostructured ZnO (Pesika, Stebe, & Searson, 2003). The absorption spectrum in Fig. 1 is also in agreement with the spectrum of AA-ZnO reported earlier (Trandafilović et al., 2012). The results of the UV–vis absorption analysis of the S-ZnO and G-ZnO were similar to that of St-ZnO and they will not be reported. However, we estimated the average size of the particles from the observed shift of the excitonic maximum using earlier proposed binding model (Bouropoulos, Tsiaoussis, Poulopoulos, Roditis, & Baskoutas, 2008; Viswanatha et al., 2004). The obtained sizes of the particles were 7.0, 6.6, 5.9 and 5.7 nm for G-ZnO, S-ZnO, St-ZnO and AA-ZnO samples, respectively, which suggests that there is a decrease in the size of the particles with increasing in saccharide molecular mass.

3.2. X-ray diffraction (XRD)

XRD patterns of G-ZnO nanocomposite and the bulk ZnO are shown in Fig. 3. The presence of carbohydrates can be observed as a broad diffraction peak at low angles in XRD graph G-ZnO sample. All the other peaks ((1 0 0), (0 0 2), (1 0 1), (1 0 2), (1 1 0), (1 0 3), (2 0 0), (1 1 2) and (2 0 1)) coincide with hexagonal (wurtzite) crystal structure of bulk ZnO (JCPDS Card No. 89-1397). With respect to the XRD lines of the bulk ZnO, the peaks of the G-ZnO sample are relatively broad due to the small size of the particles. The G-ZnO, S-ZnO and AA-ZnO nanoparticles show similar diffraction pattern so they are not included in Fig. 2. Instead, we calculated the average size of the particles in each of the samples using the Scherrer equation:

$$D_{hkl} = \frac{k\lambda}{\beta_{hkl}\cos\theta_{hkl}} \quad (2)$$

where D_{hkl} is the crystallite size perpendicular to the normal line of ($h\,k\,l$) plane, k is a constant (0.89), β_{hkl} is the full width at half maximum of the ($h\,k\,l$) diffraction peak, θ_{hkl} is the Bragg angle of ($h\,k\,l$) peak and λ is the wavelength of Cu-K_α line. The average sizes of the nanoparticles were found to be 30.9 nm, 28.3 nm, 23.6, and 19.0 nm for G-ZnO, S-ZnO, St-ZnO and AA-ZnO samples, respectively. The average size of the particles obtained using Scherrer formula is higher than that obtained from the calculations based on the optical shift, since the XRD spectrum is proportional to the mass of the particles i.e. the larger particles contribute more to the diffraction signal. In any case, a comparison of the obtained values implies again that increasing in the saccharide molecular mass leads to the decreasing in the average size of the particles. This effect is important for the interpretation of the results, since it will be shown that the properties of the fiber sheets strongly depend on the size of the saccharide capped-ZnO particles used for their modification.

3.3. Scanning electron microscopy (SEM)

The scanning electron microscope images of the unmodified (control) and ZnO-bio-nanocomposites (G-ZnO, S-ZnO, St-ZnO and AA-ZnO) incorporated cellulose fibers sheets are presented in Fig. 4. The sample surfaces were investigated in BSE mode, where the image contrast strongly depends on the atomic number of the elements in the sample. In contrast to the BSE image of the control sample (Fig. 4a), the ZnO modified sheets depict a large number of bright formations (indicated by the errors in Fig. 4b–e), which obviously contain heavier atoms than the rest of the matrix. The micrographs in Fig. 4b–e basically show that the clusters of ZnO nanoparticles are randomly dispersed on the surface of cellulose fibers.

3.4. Immobilization of the antibodies on the ZnO modified papers

For the quantification of the degree of immobilization of the antibodies a Bradford assay calibration curve was made (Fig. 1). The initial concentration of the antibodies (10 μL of antibody in 2 mL of saline) was taken as a unit (i.e. 100%) and the other points were obtained by serial dilution of the original solution. To test the degree of the immobilization of antibodies on the surface of cellulose sheets, they are rewetted with 2 mL of saline solution and the concentration of desorbed antibodies was determined using curve

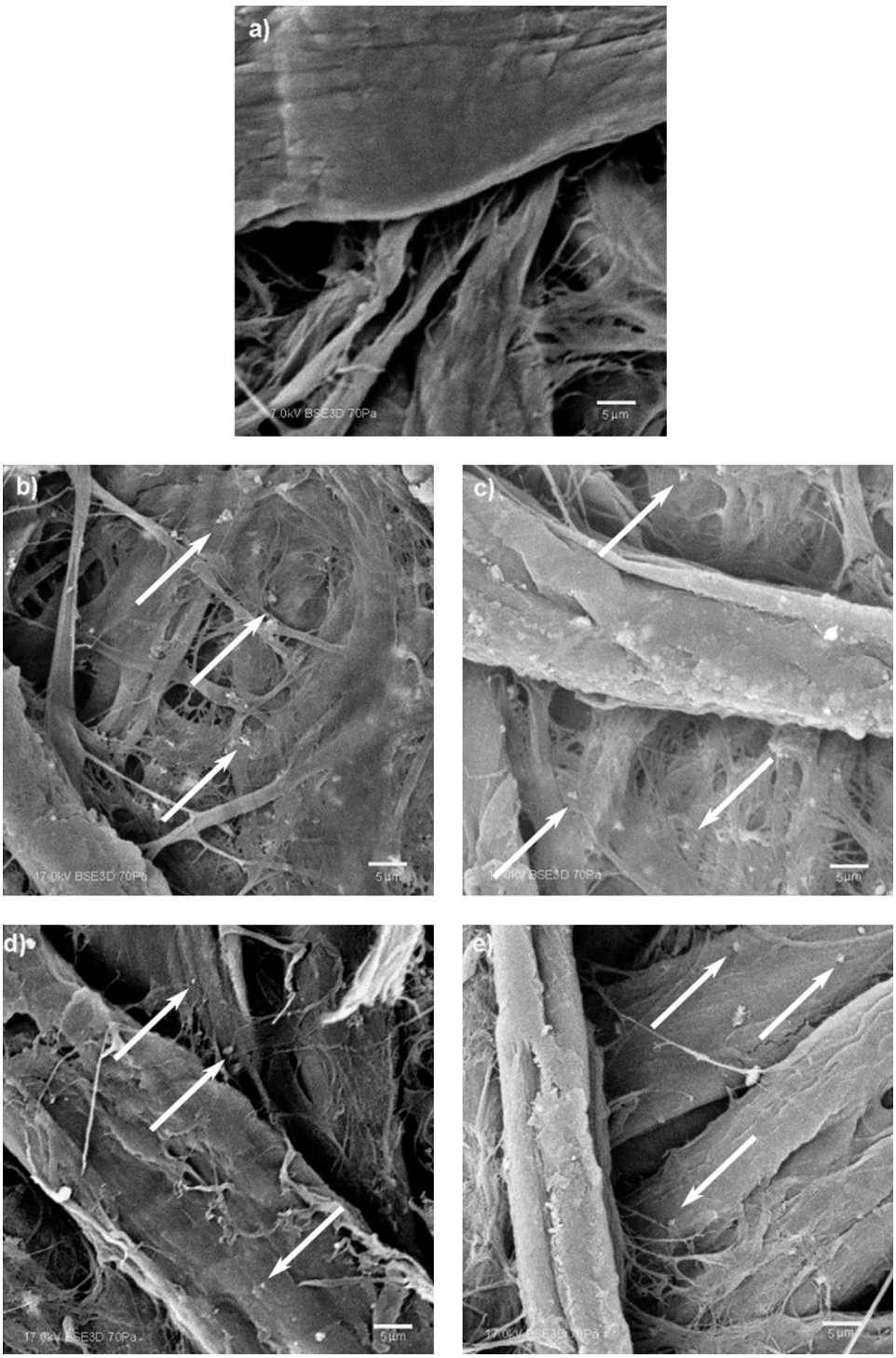

Fig. 4. SEM micrographs of (a) control and ZnO-modified cellulose fibers sheets (b) G-ZnO, (c) S-ZnO, (d) AA-ZnO and (e) St-ZnO.

in Fig. 1 (see Section 2 for details). The obtained results for control (unmodified) and ZnO-modified sheets are summarized in Table 1. The ZnO-modified cellulose fiber sheets showed higher percent retention than their unmodified counterpart. However, the highest retention was observed for the AA-ZnO sample probably due to a lower average size (higher specific surface) of the ZnO nanoparticles in this sample suggested by XRD measurements. For AA-ZnO samples, the percentages of retention of anti-A, anti-B and anti-D antibodies after saline washing were found to be 95.7%, 95.2% and 96%, respectively. This also implies that the properties of the ZnO modified sheets depend rather on the particle sizes then on the clusterization implied by SEM analysis.

The ability of the sheets to form stronger bonds with biomolecules could be of great importance for the detection of specific antigens and consequently for the application of these materials in general. In order to illustrate this, we decided to use AA-ZnO modified cellulose sheets containing anti-A, anti-B and anti-D antibodies for detection of blood types. The procedure is based on the tests found in the literature (Jarujamrus et al., 2012; Li, Tian, Al-Tamimi, & Shen, 2012) and adapted for our particular case. It is

Table 1
Percentages of retentions of antibodies of unmodified (control) and ZnO nanocomposites modified paper.

Sample (10 mm × 10 mm)		Initial amount of antibody (μl)	Retention (%)
Control	Control-A	10	49.3
	Control-B	10	50.1
	Control-D	10	49.7
G-ZnO	G-ZnO-A	10	72.7
	G-ZnO-B	10	73.2
	G-ZnO-D	10	73.8
S-ZnO	S-ZnO-A	10	76.5
	S-ZnO-B	10	76.6
	S-ZnO-D	10	76.1
St-ZnO	St-ZnO-A	10	77.7
	St-ZnO-B	10	78.5
	St-ZnO-D	10	78.9
AA-ZnO	AA-ZnO-A	10	95.7
	AA-ZnO-B	10	95.2
	AA-ZnO-D	10	96.0

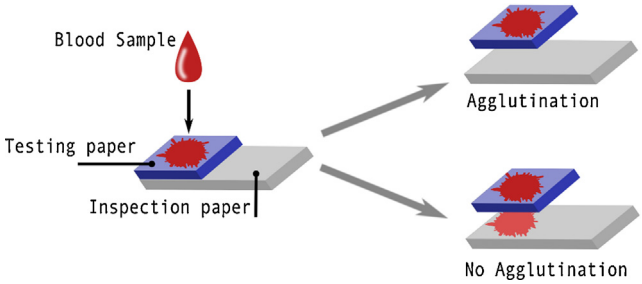

Fig. 5. A schematic diagram that describes the protocol of blood typing tests using cellulose fiber sheets.

presented schematically in Fig. 5. A drop of blood was placed on the AA-ZnO modified sheet with a particular antibody (A, B or D). The antibody-specific agglutination of red blood cells (RBCs) on cellulose sheet will not leave the stain on the inspection paper attached bellow. On the other hand, the blood stain on the inspection paper indicates that no RBCs agglutination occurred and the test is negative (Fig. 5). Using this approach we tested three different blood samples of known blood types (A^+, B^+ and AB^+). The results were shown in Fig. 6. The AA-ZnO modified sheets were marked as Sheet A, Sheet B and Sheet D depending on the type of antibody they contain. It can be seen that in the case of the first blood sample the RBCs agglutination takes place in the Sheet A (no stain) but not in Sheet B. At the same time, the absence of stain on the inspection paper after removing Sheet D suggests that the blood type is Rh positive. From this test, we confirmed that the type of the first blood sample is indeed A^+. Similarly, the other two tests imply that the blood types are B^+ and AB^+, respectively. It should be noted that

Table 2
Viable cells reduction activity of ZnO-modified fiber sheets on *Escherichia coli* and *Staphylococcus aureus* after 2 h of exposure.

Samples	*E. coli*		*S. aureus*	
	CFU	*R* (%)	CFU	*R* (%)
Control	2.12×10^5	–	1.24×10^5	–
G-ZnO	9.99×10^4	80.49	8.51×10^4	57.78
S-ZnO	7.49×10^4	85.37	6.69×10^4	66.68
St-ZnO	8.40×10^4	83.59	5.84×10^4	52.90
AA-ZnO	1.23×10^5	86.06	3.63×10^4	81.71

the paper with antibody D can sometimes give the false negative result (i.e. it can show the stain on the inspection paper) in the case of the Rh positive blood due to a weak hemagglutination reaction (Jarujamrus et al., 2012). In the mention study the degree of the retention of antibodies on the paper was about 60% and the authors had to significantly increase the concentration of D-antibodies to facilitate the antibody-antigen reaction. In our investigations, we observed similar effect, not just with Anti-D, but also with Anti-A and Anti-B antibodies when we used unmodified fiber sheets (as can be seen in Table 1 the retention of antibodies on these sheets is about 50%). On the other hand, we did not observe any false result with AA-ZnO containing cellulose sheets, although we performed a dozen of independent tests. We believe that this is related to a strong ability of AA-ZnO modified cellulose sheets to immobilize the antibodies, with the percentage of retention of more than 95% after they have been washed with saline solution (Table 1).

3.5. Antibacterial activity

ZnO is well known antimicrobial agent in the pH neutral region (pH = 7–8) with and without the presence of light (Applerot et al., 2009; Jones et al., 2008; Sawai, 2003; Stoimenov, Klinger, Marchin, & Klabunde, 2002; Yamamoto, 2001). For this reason, we decided to test the antibacterial activities of ZnO-modified cellulose sheets against common pathogens *S. aureus* and *E. coli*. The results of the antibacterial activity of the control as well as G-ZnO, S-ZnO, St-ZnO and AA-ZnO modified sheets are presented in Table 2. The cellulose sheet made from original fibers showed no activity against the tested strains, while in the presence of ZnO containing sheets the number of bacterial colonies was significantly reduced. A stronger activity was observed against *E. coli* with more than 80% of reduction (Table 2). In the case of *S. aureus*, only AA-ZnO modified sheet showed similar activity. The antibacterial effect of ZnO has been attributed to the generation of highly reactive oxygen species, particularly H_2O_2, on its surface (Applerot et al., 2009; Jun Sawai et al., 1998; Stoimenov et al., 2002; Yamamoto, 2001). The peroxide formed penetrates through the cell walls inducing fatal damage to bacteria. The fact that the *S. aureus* showed higher resistance to the antimicrobial action of ZnO in the sheets than *E. coli* is probably related to different cell wall properties of these

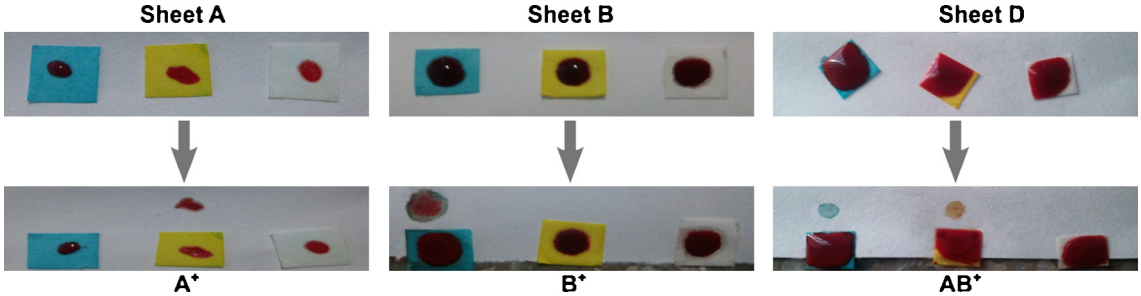

Fig. 6. Testing of blood types with AA-ZnO modified cellulose fiber sheets containing Anti A (Sheet A), Anti B (Sheet B) and Anti D (Sheet D) antibodies. All the samples showed expected RBCs agglutination, indicating that the adsorbed antibodies are capable to immobilize all RBCs.

Table 3
Tensile indices of unmodified (control) and ZnO modified fiber sheets before and after *G. trabeum* fungal infection.

Samples	Tensile index before infection (Nm/g)	Tensile index after infection (Nm/g)	% loss
Control	30.5	17.9	41.3
G-ZnO	33.6	26.9	19.9
S-ZnO	34.5	27.8	19.4
St-ZnO	33.1	27.1	18.1
AA-ZnO	35.9	30.5	15.0

two microorganisms. The cell wall of *E. coli*, which is a Gram negative bacterium, possesses a narrow layer of peptidoglycans and wide layer of lipopolysaccharides that are susceptible to oxidation (Van Heijenoort, 2001). *S. aureus* (a Gram positive bacterium) has thicker wall that contains peptidoglycans and immunostimulator molecule, lipoteichoic acid. Thick wall together with the presence of antioxidant enzymes, such as catalase, gives *S. aureus* a slightly higher oxidant resistance. Higher resistance of Gram positive with respect to Gram negative bacteria to the action of ZnO was also observed in other studies (Applerot et al., 2009; Yamamoto, 2001). Finally, it should be mention that the AA-ZnO modified fiber sheets probably show higher activity against *S. aureus* than the other samples due to a smaller average size of the particles. The creation of H_2O_2 depends on the surface area of zinc oxide, which obviously increases with decreasing in the particle sizes (Yamamoto, 2001). This argument (that the AA-ZnO modified fiber sheets show the strongest activity due to the presence of smaller particles with larger specific surfaces) is also in agreement with the highest retention of the antibodies observed for this sample (Table 1).

3.6. Antifungal activity

The organic, hydrophilic and highly porous nature of the cellulose fiber sheet makes it vulnerable to microbial attack. Here, ZnO modified fiber sheets were assessed for their tolerance toward the infection with wood-decay fungus, *G. trabeum*. The ZnO nanoparticles showed pronounced activity against the most common pathogenic yeast *Candida albicans* (Lipovsky, Nitzan, Gedanken, & Lubart, 2011) and we considered that it can also improve the resistivity of the sheets to the fungal infections. *G. trabeum* is a brown rot fungus that has the ability to depolymerize cellulose and hemicellulose without removing the lignin barrier. The unmodified and ZnO-modified fiber sheets were exposed to the fungal infection for 10 days. Fig. 7 shows the control and AA-ZnO modified sheets at the end of the period of exposure. It can be seen that the unmodified cellulose sheet is completely infected, while the ZnO containing sample is resistant to *G. trabeum*. To prove that this is indeed the case, we had to check the mechanical properties of the fiber sheets after fungal exposure and this is going to be discussed in the section below. We analysed the influence of the ZnO nanoparticles on the tensile index of the fiber sheets as well as the changes in the tensile index after the infection of the sheets with *G. trabeum*.

3.7. Mechanical properties

Table 3 shows the tensile index values of the sheets prepared from unmodified and ZnO modified fibers. The tensile indices of the sheets obviously increase after modification with ZnO nanoparticles. The highest increase in strength of almost 18% was observed in the case of the sheet modified with AA-ZnO (from 30.5 N mg^{-1} for the control sheet to 35.9 N mg^{-1}). Again, this could be a consequence of the smaller average ZnO particle sizes in this sample, which improve the inter fiber bonding. In the feature article in

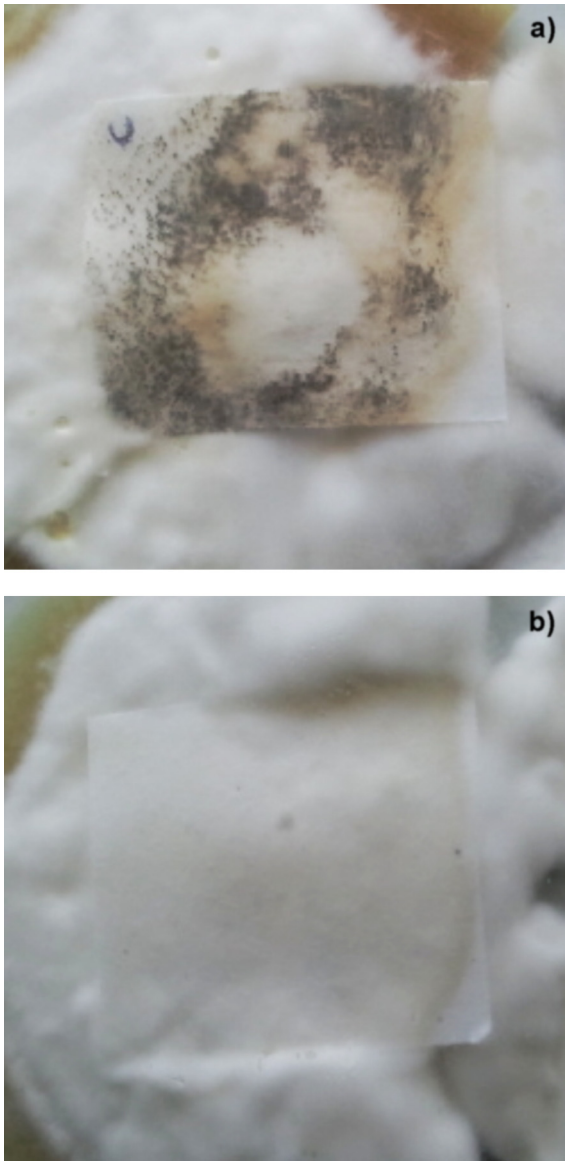

Fig. 7. Antifungal activity of unmodified (control) and AA-ZnO modified fiber sheets. The unmodified (control) sheet (a) is completely infected by fungus, while in AA-ZnO modified sheet (b) an insignificant fungus infection was observed.

TAPPI Journal, Cowan (1995) argued that the tensile strength of the paper depends on several factors. They include the average load-bearing ability of the individual fibers, the number of fibers at any given cross-section available for load transfer and the uniformity of the load transfer that is allowed by the network structure. Since the fiber network is intrinsically inhomogeneous, we believe that ZnO nanoparticles act as bonding agents that improve fiber-fiber interaction and consequently increase the ability of network to withstand the applied load. Similar effect was observed in our previous study (Csóka et al., 2012), where silver nanoparticles were used in the fabrication of antimicrobial paper. It should also be noted that our laboratory sheet former produced the sheets with random orientation of the fibers and consequently isotropic mechanical properties. In order to minimize the effects of moisture and temperature papers are conditioned at 23 °C and 50% relative humidity (RH) prior to measurements. Finally, the mechanical properties of the paper can depend on its grammage and for this reason we reported tensile indices of the sheets in Table 3 instead of their tensile strengths.

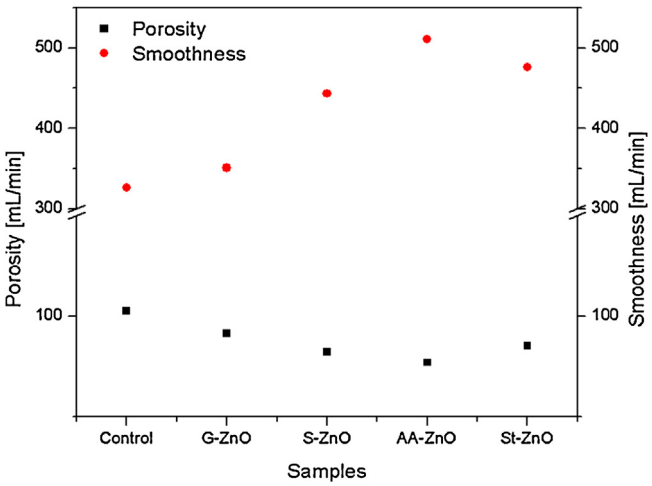

Fig. 8. Porosity and smoothness of unmodified (control) and ZnO-modified fiber sheets.

The tensile indices were also used for the quantifiable analysis of anti-fungal activity discussed above. The effects of the exposure to *G. trabeum* will be reflected in the altered mechanical behavior of the sheets. The tensile indices of the unmodified and ZnO modified sheets after fungal infection are also presented in Table 3. In the fourth column of Table 3, we stated the percentage losses in tensile indices after the exposure. After 10 days of exposure, the tensile index of the unmodified (control) sheet lost 41.3% from its initial value, while this effect was less pronounced in ZnO-modified cellulose sheets. The minimum loss of 15% was observed in the case of AA-ZnO-modified papers (Table 3).

Although the main goal of this study was to make bioactive paper, the results presented above showed that modification with G-ZnO, S-ZnO, St-ZnO and AA-ZnO nanoparticles improve the mechanical and anti-fungal properties of the sheets. As it will be seen in the next sections, the ZnO nanoparticles also affect the other important properties the sheets such as the porosity, smoothness, brightness and opacity.

3.8. Porosity and smoothness

The smoothness of a paper relates to the shortness and slenderness of the cellulose fibers used and the degree of "filling in" of fiber on the surface (Fang et al., 2013; Ray & Tyagi, 2012). High smoothness is important for writing paper, where it affects the ease of travel of a pen, as well as for all types of printing and photographic papers for clarity of the images. The smoothness is affected by the raw material selection, its processing and coating. Smoothening of the paper is usually achieved by increasing the calendar pressure which is, on the other hand, followed by decreasing in the thickness or bulk of the paper (the inverse of density). We tested the porosity and smoothness on the control and various ZnO modified sheets. The results were presented in Fig. 8. It was found that the incorporation of ZnO nanoparticles substantially decreased the porosity of the cellulose sheets from 102.6 mL/min (control) to 77 mL/min (AA-ZnO). At the same time, the smoothness value increases from 326 mL/min (control) to 511 mL/min in the case of the AA-ZnO modified sheet. The modification of the fibers with G-ZnO, S-ZnO, St-ZnO influences the porosity/smoothness of the sheets in a similar way but to a lesser extent (Fig. 8). The saccharide modified ZnO nanoparticles obviously show the ability to reduce the volume of the voids within the fibrous structure. This effect of increasing in smoothness by incorporation of ZnO nanoparticles is very important for the application of these materials, considering that some printing techniques were employed in the fabrication of bioactive papers (Abe et al., 2008; Hossain et al., 2009; Li et al., 2012). For example, the composite text patterns (comprising the bioactive and nonbioactive sections) were printed on the surface of the papers, which are then able to form the letters and symbols for the final display of the testing report (Li et al., 2012).

Table 4
Brightness and opacity of unmodified (control) and ZnO-modified fiber sheets.

Samples	Brightness (% ISO)	Opacity
Control	82.0	88.3
G-ZnO	82.0	88.9
S-ZnO	82.1	89.6
St-ZnO	79.8	89.9
AA-ZnO	82.0	93.1

3.9. Brightness and opacity

No substantial changes in the brightness were observed when saccharide capped ZnO nanoparticles were incorporated into the cellulose sheets (Table 4). The brightness of AA-ZnO treated sheet slightly decreased probably due to pale yellow color of the alginic acid. On the other hand, the G-ZnO, S-ZnO, St-ZnO and AA-ZnO modified samples show higher opacity values than the control sheet. There is a significant increase in the opacity from 88.3 to 93.1 in the case of St-ZnO treated sheets (Table 4). This implies that the ZnO nanoparticles were more uniformly distributed within the fiber network, probably due to a specific interaction of the corresponding saccharides and polysaccharides with cellulose fibers prior to the formation of the sheets.

4. Conclusion

Impregnation of cellulose fiber sheets with saccharide capped ZnO nanoparticles has a profound effect on their physical properties. Four saccharides (glucose, sucrose, starch and alginic acid) were used as controlled environments for the growth of nanostructured ZnO. The particles with the smallest average size were obtained in the presence of polysaccharide alginic acid (AA) and, for this reason, the most pronounced changes in the properties of the sheets were observed after modification of the cellulose fibers with this sample (AA-ZnO). The ZnO-modified cellulose fiber sheets showed a high ability to immobilize antibodies (biomolecules) on their surfaces. In the case of AA-ZnO treated sheet, the degree of retention of antibodies after washing with saline solution was about 95%. A high level of retention makes these fiber sheets suitable for various biomedical applications and we confirmed the proof of concept on the detection of the blood types using Anti-A, Anti-B and Anti-D antibodies. The presence ZnO nanoparticles also provide antimicrobial and antifungal properties to the fiber sheets. They reduced the number of colonies of pathogen bacteria (*E. coli* and *S. aureus*) and improved the resistance of the cellulose sheets toward the attack of wood-decay fungus, *G. trabeum*.

The ZnO nanoparticles facilitate inter-fiber bonding, which induced changes in tensile strength, smoothness and porosity of the sheets. The tensile index of the AA-ZnO modified sheet increased by 18% compared to that of the control sample. The incorporation of ZnO nanoparticles reduced the porosity of the cellulose sheets (from 102.6 mL/min (control) to 77 mL/min (AA-ZnO)) and improved their smoothness (from 326 mL/min (control) to 511 mL/min (AA-ZnO)). Finally, the modification with ZnO nanoparticles did not affect significantly the brightness but it increased the opacity of the sheets. A general conclusion is that the present approach enables preparation of multifunctional cellulose sheets for high-end applications such as antimicrobial and bioactive paper.

Acknowledgments

This study was supported by the Environment conscious energy efficient building TAMOP-4.2.2.A-11/1/KONV-2012-0068 project sponsored by the EU and European Social Foundation and by the Ministry of Education, Science and Technological Development of the Republic of Serbia (Project Nos. 172056 and 45020).

References

Abe, K., Suzuki, K., & Citterio, D. (2008). Inkjet-printed microfluidic multianalyte chemical sensing paper. *Analytical Chemistry*, *80*, 6928–6934.

Ali, M. M., Aguirre, S. D., Xu, Y., Filipe, C. D. M., Pelton, R., & Li, Y. (2009). Detection of DNA using bioactive paper strips. *Chemical Communications*, 6640–6642.

Applerot, G., Lipovsky, A., Dror, R., Perkas, N., Nitzan, Y., Lubart, R., et al. (2009). Enhanced antibacterial activity of nanocrystalline ZnO due to increased ROS-mediated cell injury. *Advanced Functional Materials*, *19*(6), 842–852.

Ashour, A., Kaid, M., Elsayed, N., & Ibrahim, A. (2006). Physical properties of ZnO thin films deposited by spray pyrolysis technique. *Applied Surface Science*, *252*, 7844–7848.

Bouropoulos, N., Tsiaoussis, I., Poulopoulos, P., Roditis, P., & Baskoutas, S. (2008). ZnO controllable sized quantum dots produced by polyol method: An experimental and theoretical study. *Materials Letters*, *62*, 3533–3535.

Bozanic, D. K., Dimitrijevic-Brankovic, S., Bibic, N., Luyt, A. S., & Djokovic, V. (2011). Silver nanoparticles encapsulated in glycogen biopolymer: Morphology, optical and antimicrobial properties. *Carbohydrate Polymers*, *83*, 883–890.

Bozanic, D. K., Djokovic, V., Blanusa, J., Nair, P. S., Georges, M. K., & Radhakrishnan, T. (2007). Preparation and properties of nano-sized Ag and Ag_2S particles in biopolymer matrix. *European Physical Journal E*, *22*, 51–59.

Božanić, D. K., Luyt, A. S., Trandafilović, L. V., & Djoković, V. (2013). Glycogen and gold nanoparticle bioconjugates: Controlled plasmon resonance via glycogen-induced nanoparticle aggregation. *RSC Advances*, *3*, 8705–8713.

Brida, D., Fortunato, E., Águas, H., Silva, V., Marques, A., Pereira, L., et al. (2002). New insights on large area flexible position sensitive detectors. *Journal of Non-Crystalline Solids*, *299–302*, 1272–1276.

Chang, P. R., Yu, J., & Ma, X. (2009). Fabrication and characterization of Sb_2O_3/carboxymethyl cellulose sodium and the properties of plasticized starch composite films. *Macromolecular Materials and Engineering*, *294*, 762–767.

Chang, P. R., Yu, J., Ma, X., & Anderson, D. P. (2011). Polysaccharides as stabilizers for the synthesis of magnetic nanoparticles. *Carbohydrate Polymers*, *83*, 640–644.

Cowan, W. F. (1995). High-shear laboratory beating and fiber-quality testing offer new insights into pulp evaluation. *TAPPI Journal*, *78*, 133–137.

Csóka, L., Božanić, D. K., Nagy, V., Dimitrijević-Branković, S., Luyt, A. S., Grozdits, G., et al. (2012). Viscoelastic properties and antimicrobial activity of cellulose fiber sheets impregnated with Ag nanoparticles. *Carbohydrate Polymers*, *90*, 1139–1146.

Fang, Z., Zhu, H., Preston, C., Han, X., Li, Y., Lee, S., et al. (2013). Highly transparent and writable wood all-cellulose hybrid nanostructured paper. *Journal of Materials Chemistry C*, *1*, 6191–6197.

Ghule, K., Ghule, A. V., Chen, B.-J., & Ling, Y.-C. (2006). Preparation and characterization of ZnO nanoparticles coated paper and its antibacterial activity study. *Green Chemistry*, *8*, 1034–1041.

Gottesman, R., Shukla, S., Perkas, N., Solovyov, L. A., Nitzan, Y., & Gedanken, A. (2011). Sonochemical coating of paper by microbiocidal silver nanoparticles. *Langmuir*, *27*, 720–726.

Hossain, S. M. Z., Luckham, R. E., Smith, A. M., Lebert, J. M., Davies, L. M., Pelton, R. H., et al. (2009). Development of a bioactive paper sensor for detection of neurotoxins using piezoelectric inkjet printing of sol–gel-derived bioinks. *Analytical Chemistry*, *81*, 5474–5483.

Jain, S., Li, L., Breedveld, V., Hess, D. W., Barnett, C., Davis, M., et al. (2013). *Superhydrophobic paper influence on bacterial attachment suggests potential application as packaging material. Advanced materials. CNTs, particles, films and composites* (Vol. 1).

Jarujamrus, P., Tian, J., Li, X., Siripinyanond, A., Shiowatana, J., & Shen, W. (2012). Mechanisms of red blood cells agglutination in antibody-treated paper. *Analyst*, *137*, 2205–2210.

Jones, N., Ray, B., Ranjit, K. T., & Manna, A. C. (2008). Antibacterial activity of ZnO nanoparticle suspensions on a broad spectrum of microorganisms. *FEMS Microbiology Letters*, *279*, 71–76.

Khan, M. S., Haniffa, S. B. M., Slater, A., & Garnier, G. (2010). Effect of polymers on the retention and aging of enzyme on bioactive papers. *Colloids and Surfaces B: Biointerfaces*, *79*, 88–96.

Li, M., Tian, J., Al-Tamimi, M., & Shen, W. (2012). Paper-based blood typing device that reports patient's blood type in Writing. *Angewandte Chemie International Edition*, *51*, 5497–5501.

Li, X., Tian, J., Nguyen, T., & Shen, W. (2008). Paper-based microfluidic devices by plasma treatment. *Analytical Chemistry*, *80*, 9131–9134.

Lipovsky, A., Nitzan, Y., Gedanken, A., & Lubart, R. (2011). Antifungal activity of ZnO nanoparticles-the role of ROS mediated cell injury. *Nanotechnology*, *22*, 105101.

Moos, P. J., Olszewski, K., Honeggar, M., Cassidy, P., Leachman, S., Woessner, D., et al. (2011). Responses of human cells to ZnO nanoparticles: A gene transcription study. *Metallomics: Integrated Biometal Science*, *3*, 1199–1211.

Murugadoss, A., & Chattopadhyay, A. (2008). A green chitosan–silver nanoparticle composite as a heterogeneous as well as micro-heterogeneous catalyst. *Nanotechnology*, *19*, 015603.

Pancek, A., Kvitek, L., Prucek, R., Kolar, M., Vecerova, R., Pizurova, N., et al. (2006). Silver colloid nanoparticles: Synthesis, characterization, and their antibacterial activity. *Journal of Physical Chemistry B*, *110*, 16248–16253.

Perelshtein, I., Ruderman, E., Perkas, N., Tzanov, T., Beddow, J., Joyce, E., et al. (2013). Chitosan and chitosan–ZnO-based complex nanoparticles: Formation, characterization, and antibacterial activity. *Journal of Materials Chemistry B*, 1968–1976.

Pesika, N. S., Stebe, K. J., & Searson, P. C. (2003). Relationship between absorbance spectra and particle size distributions for quantum-sized nanocrystals. *Journal of Physical Chemistry B*, *107*, 10412–10415.

Prasad, V., Shaikh, A. J., Kathe, A. A., Bisoyi, D. K., Verma, A. K., & Vigneshwaran, N. (2010). Functional behaviour of paper coated with zinc oxide–soluble starch nanocomposites. *Journal of Materials Processing Technology*, *210*, 1962–1967.

Radhakrishnan, T., Georges, M. K., Nair, P. S., Luyt, A. S., & Djoković, V. (2007). Study of Sago starch–CdS nanocomposite films: Fabrication, structure, optical and thermal properties. *Journal of Nanoscience and Nanotechnology*, *7*, 986–993.

Raveendran, P., Fu, J., & Wallen, S. L. (2003). Completely green synthesis and stabilization of metal nanoparticles. *Journal of the American Chemical Society*, *125*, 13940–13941.

Ray, A. K., & Tyagi, S. (2012). Validation of calendering models for coated papers made from blend of agri-residue and softwood pulp with softnip calendering techniques. In *AIChE Annual Meeting, Pittsburgh, PA*. Code 94591.

Sawai, J. (2003). Quantitative evaluation of antibacterial activities of metallic oxide powders (ZnO, MgO and CaO) by conductimetric assay. *Journal of Microbiological Methods*, *54*, 177–182.

Sawai, J., Shoji, S., Igarashi, H., Hashimoto, A., Kokugan, T., Shimizu, M., et al. (1998). Hydrogen peroxide as an antibacterial factor in zinc oxide powder slurry. *Journal of Fermentation and Bioengineering*, *86*, 521–522.

Shih, C.-M., Shieh, Y.-T., & Twu, Y.-K. (2009). Preparation of gold nanopowders and nanoparticles using chitosan suspensions. *Carbohydrate Polymers*, *78*, 309–315.

Stoimenov, P. K., Klinger, R. L., Marchin, G. L., & Klabunde, K. J. (2002). Metal oxide nanoparticles as bactericidal agents. *Langmuir*, *18*, 6679–6686.

Thorp, B. A., & Kocurek, M. J. (1991). *Strength properties. Pulp and paper manufacture: Paper machine operation* (Vol. 7) Atlanta: Tappi.

Trandafilović, L. V., Božanić, D. K., Dimitrijević-Branković, S., Luyt, A. S., & Djoković, V. (2012). Fabrication and antibacterial properties of ZnO–alginate nanocomposites. *Carbohydrate Polymers*, *88*, 263–269.

Umar, A., Rahman, M. M., Al-Hajry, A., & Hahn, Y.-B. (2009). Highly-sensitive cholesterol biosensor based on well-crystallized flower-shaped ZnO nanostructures. *Talanta*, *78*, 284–289.

Van Heijenoort, J. (2001). Formation of the glycan chains in the synthesis of bacterial peptidoglycan. *Glycobiology*, *11*, 25R–36R.

Vigneshwaran, N., Kumar, S., Kathe, A. A., Varadarajan, P. V., & Prasad, V. (2006). Functional finishing of cotton fabrics using zinc oxide–soluble starch nanocomposites. *Nanotechnology*, *17*, 5087–5095.

Viswanatha, R., Sapra, S., Satpati, B., Satyam, P. V., Dev, B. N., & Sarma, D. D. (2004). Understanding the quantum size effects in ZnO nanocrystals. *Journal of Materials Chemistry*, *14*, 661–668.

Walsh, D., Arcelli, L., Ikoma, T., Tanaka, J., & Mann, S. (2003). Dextran templating for the synthesis of metallic and metal oxide sponges. *Nature Materials*, *2*, 386–390.

Wang, Z. L. (2004). Zinc oxide nanostructures: Growth, properties and applications. *Journal of Physics: Condensed Matter*, *16*, R829–R858.

Yamamoto, O. (2001). Influence of particle size on the antibacterial activity of zinc oxide. *International Journal of Inorganic Materials*, *3*, 643–646.

Yu, J., Yang, J., Liu, B., & Ma, X. (2009). Preparation and characterization of glycerol plasticized-pea starch/ZnO-carboxymethylcellulose sodium nanocomposites. *Bioresource Technology*, *100*, 2832–2841.